Journal of Organometallic Chemistry 705 (2012) 51–58

Contents lists available at SciVerse ScienceDirect

Journal of Organometallic Chemistry

journal homepage: www.elsevier.com/locate/jorganchem

Polymerization of 1,3-butadiene catalyzed by cobalt(II) and nickel(II) complexes bearing imino- or amino-pyridyl alcohol ligands in combination with ethylaluminum sesquichloride

Pengfei Ai, Lin Chen, Yintian Guo, Suyun Jie*, Bo-Geng Li*

State Key Laboratory of Chemical Engineering, Department of Chemical and Biological Engineering, Zhejiang University, 38 Zheda Road, Hangzhou 310027, China

ARTICLE INFO

Article history:
Received 30 November 2011
Received in revised form
10 January 2012
Accepted 17 January 2012

Keywords:
Cobalt
Nickel
1,3-Butadiene
Polymerization

ABSTRACT

A series of cobalt(II) (**1a**–**6a**) and nickel(II) (**1b**–**6b**) complexes supported by imino- or amino-pyridyl alcohol ligands (tridentate [NNO]), 2-(2,6-$R^1{}_2C_6H_3N{=}CMe$)-6-{$(HO)CR_2$}C_5H_3N (**L1**–**L4**) and 2-(2,6-$R^1{}_2C_6H_3NHCHMe$)-6-$(CH_2OH)C_5H_3N$ (**L5** and **L6**), were synthesized and characterized by elemental and spectroscopic analysis along with X-ray diffraction analysis. The X-ray diffraction demonstrated that all the complexes adopted distorted trigonal bipyramidal configuration with the equatorial plane formed by the pyridyl nitrogen atom and two chlorine atoms. On activation with ethylaluminum sesquichloride (EASC), the cobalt complexes (**1a**–**6a**) displayed high catalytic activity for the polymerization of 1,3-butadiene to yield *cis*-1,4-polybutadiene with high selectivity (>96%) under the Al/Co molar ratio of 40 at 25 °C. The conversion of butadiene, microstructure and molecular weight of the resulting polymers were affected by the reaction parameters and ligand environment. However, in comparison with the corresponding cobalt complexes, the nickel complexes (**1b**–**6b**) obtained relatively lower catalytic activity, *cis*-1,4 content and molecular weight under the similar reaction conditions.

1. Introduction

Polybutadienes (PBDs) are formed via 1,4- or 1,2-insertions, which lead to *cis*-1,4, *trans*-1,4 or 1,2-vinyl microstructures. Among these different isomers, high *cis*-1,4-PBD has obtained much industrial importance due to its natural-rubber-like properties [1], which is produced commercially by the solution polymerization of 1,3-butadiene with the Ziegler–Natta catalysts based on transition metals or rare earth metals, such as $TiC1_4/I_2/Al(i\text{-}Bu)_3$ [2], $CoCl_2/AlEt_2Cl$ [1b,3], $Ni(OOCR)_2/BF_3{\cdot}OEt_2/AlEt_3$ [4], or $Nd(OOCR)_3/Et_3Al_2Cl_3/Al(i\text{-}Bu)_2H$ [5] in aromatic or aliphatic hydrocarbons at 50–70 °C. The cobalt-based catalysts have been widely investigated probably because they can produce PBDs with different microstructures, including *cis*-1,4-PBD and syndiotactic 1,2-PBD depending on the polymerization parameters and catalyst structure. The halides and carboxylates of cobalt are stereoselective to high *cis*-1,4-PBD when activated with methylaluminoxane (MAO) [6]. However, the cobalt halides when combined with alkylphosphines or pyridyl adducts produced predominantly 1,2-PBD [7]. The nickel-based catalysts are also of particular interest in the production of high *cis*-1,4-PBD since the resulting PBDs have good processing properties and high tack due to broad molecular weight distribution and many branches [8].

In the polymerization of butadiene with transition metal catalysts, the ligand structures play an important role in determining both the catalytic activity and the microstructures of PBDs. Cobalt complexes bearing bi-, tri- or multi-dentate organic ligands have been used as catalysts in the polymerization of butadiene. For example, four-coordinated (salen)cobalt(II) ($[ONNO]^{2-}$) [9] and bis(salicylaldiminate)cobalt(II) complexes ($[NO]^-$) [10], five-coordinated cobalt dichloride complexes bearing neutral tridentate ligands (especially such as bis(imino)pyridine ligands [11], bis(benzimidazolyl)amine ligands [12], bis(benzimidazolyl)pyridine ligands [13]) have achieved high activity and high *cis*-1,4 selectivity in the polymerization of butadiene in combination with MAO or EASC. As for nickel catalysts, (salen)nickel(II) ($[ONNO]^{2-}$) [14], nickel-tropolonoide and nickel-1,3-propanedionate ($[OO]^-$) [15] complexes have produced high conversions of butadiene with high *cis*-1,4 content in the polymers. Whereas nickel dihalide complexes bearing neutral α-dimine ligands ([NN]) [14,16] or bis(imino)pyridine ligands ([NNN]) [11b,15] were less active for the polymerization of butadiene.

During the exploration of new effective chelate metal complexes for the stereospecific polymerization of butadiene, we have found

* Corresponding authors. Tel.: +86 571 87951515; fax: +86 571 87951612.
E-mail addresses: jiesy@zju.edu.cn (S. Jie), bgli@zju.edu.cn (B.-G. Li).

0022-328X/$ – see front matter © 2012 Elsevier B.V. All rights reserved.
doi:10.1016/j.jorganchem.2012.01.013

that dinuclear cobalt(II) complexes bearing 3-aryliminomethyl-2-hydroxybenzaldehyde ligands ([NOO]) were highly active and produced high contents of *cis*-1,4-PBD by using low amount of EASC as cocatalyst [17]. Thus it would be of interest to investigate the tridentate [NNO] ligands; therefore 2-arylimino-6-(alcohol)pyridines were chosen since their nickel and cationic palladium complexes showed high catalytic activities for the vinyl polymerization of norbornene [18]. Herein we will report the synthesis and characterization of cobalt and nickel complexes bearing 2-arylimino- or 2-arylamino-6-(alcohol)pyridine ligands and their application in the stereospecific polymerization of 1,3-butadiene to produce mainly *cis*-1,4-PBD in combination with ethylaluminum sesquichloride (EASC).

2. Results and discussion

2.1. Synthesis of imino- or amino-pyridyl alcohol ligands and their complexes

The starting materials, 2-carboxylate-6-iminopyridine compounds, 2-COOEt-6-(2,6-$R^1{}_2C_6H_3N{=}CMe)C_5H_3N$ (R^1 = Me, **1**; Et, **2**; *i*-Pr, **3**) [19], were readily prepared by the condensation reaction of 6-acetylpyridine-2-carboxylate and the corresponding substituted anilines. The desired (imino)pyridyl alcohol ligand, 2-(2,6-$Et_2C_6H_3N{=}CMe)$6-{(HO)CMe_2}C_5H_3N (**L4**), was prepared by the reaction of 2.0 equiv. of MeLi with compound **2** according to the literature procedure (Scheme 1) [18,20,21]. The ligands, 6-CH_2OH-2-(2,6-$R^1{}_2C_6H_3N{=}CMe)C_5H_3N$ (R^1 = Me, **L1**; Et, **L2**; *i*-Pr, **L3**) were prepared via the reduction of compound **1**–**3** by 1.1 equiv. of sodium borohydride with the assistance of calcium chloride in methanol in good yield (Scheme 1) [18]. It is unexpected that the C=N double bonds (imino groups) in compound **1** and **2** could be also reduced to amino groups with the increased amount of sodium borohydride, leading to the formation of ligands **L5** and **L6** (Scheme 1). However, this reaction didn't occur for the 2,6-diisopropyl-substituted compound **3** despite of the addition of more excess of sodium borohydride, which was probably ascribed to more bulkiness of isopropyl groups than methyl and ethyl groups at the *ortho*-positions of imino-N aryl ring. The ligands, **L1**, **L2**, **L5** and **L6**, were identified on the basis of FT-IR, ^{1}H and ^{13}C NMR spectra as well as elemental analysis.

The 2-arylimino-6-(alcohol)pyridines (**L1**–**L4**) or 2-arylamino-6-(alcohol)pyridines (**L5** and **L6**) reacted with one equiv. of $CoCl_2{\cdot}6H_2O$ or $NiCl_2{\cdot}6H_2O$ in absolute ethanol at room temperature to yield the corresponding cobalt complexes **1a**–**6a** and nickel complexes **1b**–**6b** as air-stable powders (Scheme 2). All the complexes were characterized by FT-IR spectra and elemental analysis. In the FT-IR spectra, the stretching vibration bands of C=N

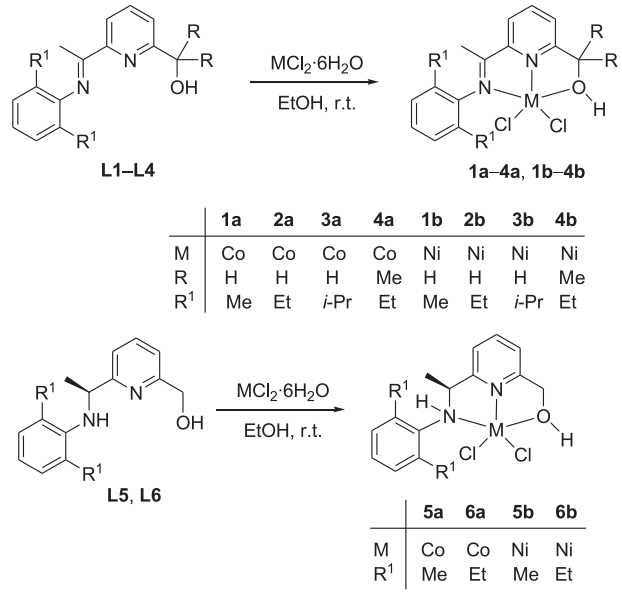

	1a	2a	3a	4a	1b	2b	3b	4b
M	Co	Co	Co	Co	Ni	Ni	Ni	Ni
R	H	H	H	Me	H	H	H	Me
R^1	Me	Et	*i*-Pr	Et	Me	Et	*i*-Pr	Et

	5a	6a	5b	6b
M	Co	Co	Ni	Ni
R^1	Me	Et	Me	Et

Scheme 2. Synthesis of cobalt complexes **1a**–**6a** and nickel complexes **1b**–**6b**.

double bonds of cobalt complexes (**1a**–**4a**) (1618–1624 cm^{-1}) and nickel complexes (**1b**–**4b**) (1616–1621 cm^{-1}) apparently shifted to lower wave number and the peak intensity greatly reduced, as compared to the corresponding free ligands (1644–1645 cm^{-1}), indicating the coordination interaction between the imino nitrogen atom and the metal center. The stretching vibration bands of all the hydroxyl groups and amino groups in complexes **5a**, **6a**, **5b** and **6b** also shifted to lower wave number than those in the free ligands. All the data of elemental analysis were in accordance with the theoretical calculations. The unambiguous structures were further confirmed by the single-crystal X-ray diffraction analysis.

2.2. Crystal structures

Single-crystals of complexes **2a** (blue), **4a** (dark green), **6a** (bright blue) and **6b** (brown) suitable for X-ray diffraction analysis were individually obtained by slow diffusion of diethyl ether into their methanol solutions. According to their structures, the coordination geometry around the cobalt or nickel center can be described as a distorted trigonal bipyramidal, in which the nitrogen atom of pyridyl group (N1) and two chlorides (Cl1 and Cl2) compose an equatorial plane. Their crystal structures are shown in Figs. 1–4, respectively, and the selected bond lengths and angles are collected in Table 1.

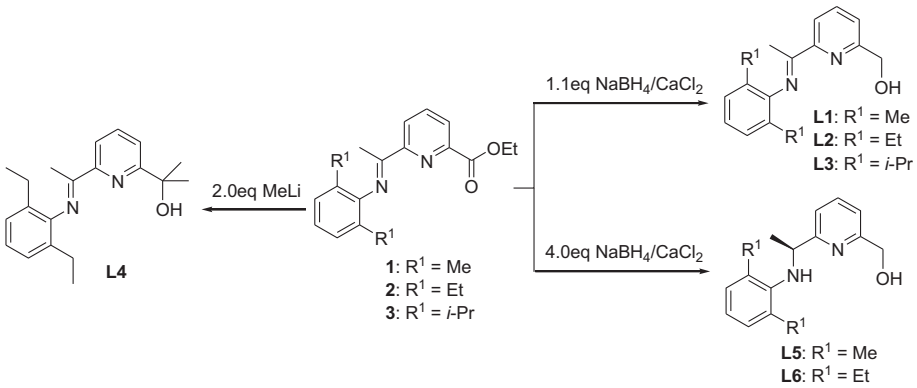

Scheme 1. Synthesis of ligands **L1**–**L6**.

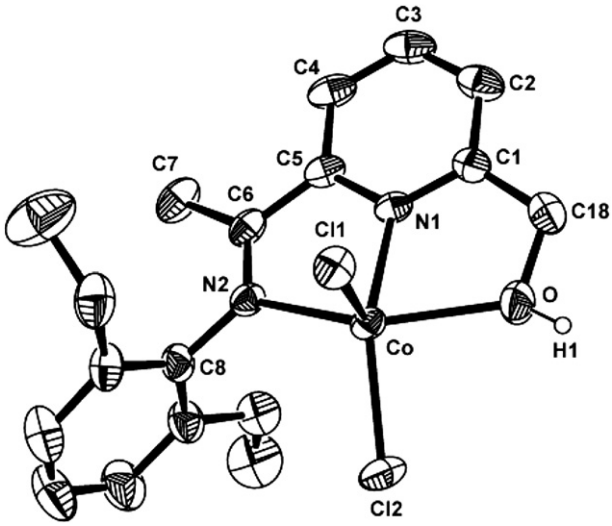

Fig. 1. Molecular structure of complex **2a** with thermal ellipsoids at the 30% probability level. Hydrogen atoms (apart from H1) have been omitted for clarity.

In the structure of **2a** (Fig. 1), the cobalt atom deviates by 0.1290 Å from the triangular plane of N1, Cl1 and Cl2 with the equatorial angle ranging from 101.34(8)° to 142.88(9)°. The axial Co–N2 and Co–O bonds subtend an angle of 145.93(12)° (O–Co–N2). The equatorial plane is nearly perpendicular to the pyridyl plane with a dihedral angle of 92.2°. The dihedral angle between the phenyl ring and the pyridyl plane is 84.4°. The Co–N1(pyridyl) bond (2.044(3) Å) in the equatorial plane is shorter than the axial Co–N2(imino) (2.149(3) Å) and Co–O (2.219(3) Å) bonds, which is similar to the corresponding iron and nickel complexes [18,20]. The two Co–Cl bond lengths show a slight difference between Co–Cl1 (2.3085(11) Å) and Co–Cl2 (2.2383(13) Å). The imino C6–N2 bond length is 1.285(5) Å with the typical character of a C=N double bond. The structure of complex **4a** (Fig. 2) with two *gem*-methyl groups on the C18 atom is similar to that of **2a**. Therefore, only the structure of **2a** was discussed in detail here.

The cobalt complex **6a** and nickel complex **6b** with the reduced (amino)pyridinyl ligand show very similar geometries and structural parameters (Table 1 and Figs. 3 and 4) and only the structure of **6a** will be discussed below, in order to compare with the corresponding complex **2a** with the(imino)pyridinyl ligand. The pyridyl nitrogen atom (N1) and two chlorides form the equatorial plane with the slight deviation of cobalt atom by 0.0323 Å from this plane. The bond angles around the cobalt center are in the range of 76.08(7)° (O–Co–N1) to 154.65(6)° (O–Co–N2). The dihedral angles between the equatorial plane and the pyridyl plane, and the phenyl ring and the pyridyl plane, are 83.6° and 97.1°, respectively. The Co–N2(amino) bond distance (2.2572(17) Å) in **6a** is longer by about 0.11 Å than that of Co–N2(imino) bond (2.149(3) Å) in **2a**, and longer by about 0.23 Å than that of the Co–N1 bond (2.0263(17) Å) in the equatorial plane. The two Co–Cl bond distances are similar. The bond length of C6–N2 is 1.496(3) Å in the range of C–N single bond, indicating the reduction of imino group to amino group.

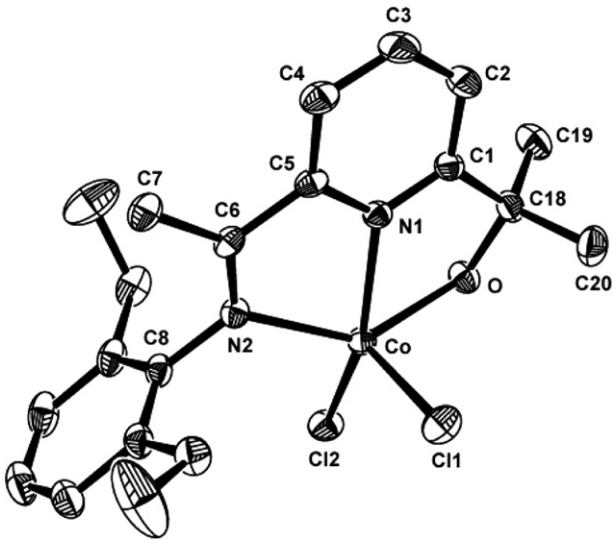

Fig. 2. Molecular structure of complex **4a** with thermal ellipsoids at the 30% probability level. All hydrogen atoms have been omitted for clarity.

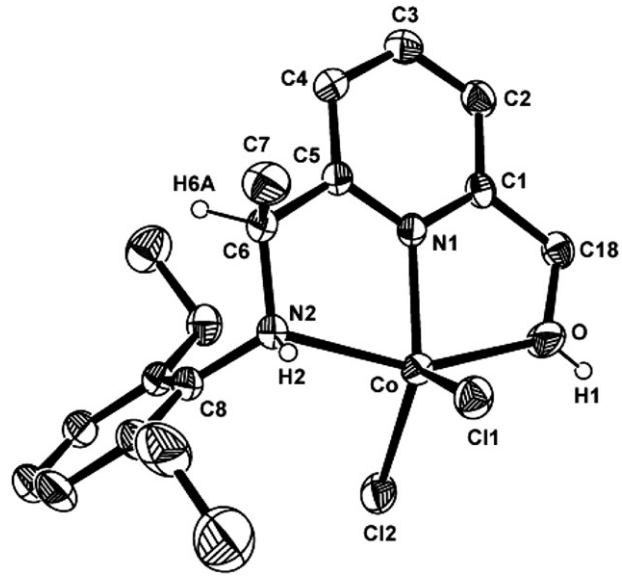

Fig. 3. Molecular structure of complex **6a** with thermal ellipsoids at the 30% probability level. Hydrogen atoms (apart from H1, H2 and H6A) have been omitted for clarity.

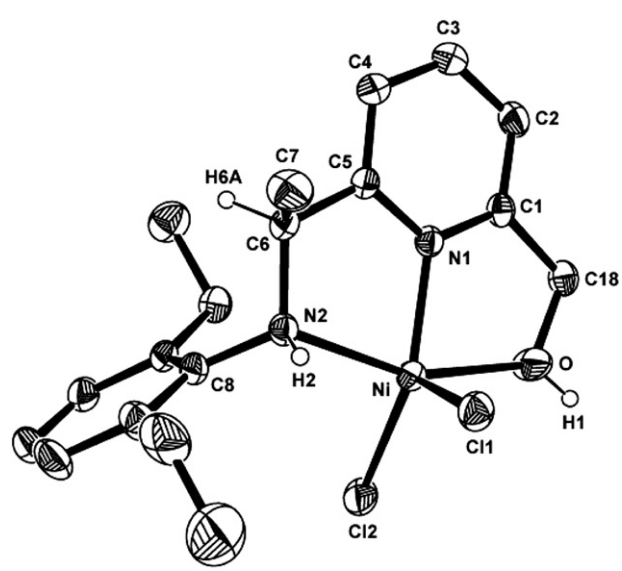

Fig. 4. Molecular structure of complex **6b** with thermal ellipsoids at the 30% probability level. Hydrogen atoms (apart from H1, H2 and H6A) have been omitted for clarity.

Table 1
Selected bond lengths (Å) and angles (°) of complexes **2a**, **4a**, **6a** and **6b**.

	2a (M = Co)	**4a** (M = Co)	**6a** (M = Co)	**6b** (M = Ni)
Bond lengths				
M–N1	2.044(3)	2.0810(15)	2.0263(17)	1.9877(19)
M–N2	2.149(3)	2.1459(14)	2.2572(17)	2.1686(18)
M–Cl1	2.3085(11)	2.3111(7)	2.2935(8)	2.3055(8)
M–Cl2	2.2383(13)	2.2781(8)	2.2595(8)	2.2535(9)
M–O	2.219(3)	2.1939(13)	2.1443(17)	2.1035(18)
C6–N2	1.285(5)	1.283(2)	1.496(3)	1.505(3)
Bond angles				
O–M–N1	72.99(12)	73.36(5)	76.08(7)	76.93(7)
O–M–N2	145.93(12)	140.61(5)	154.65(6)	157.56(7)
O–M–Cl1	97.83(10)	93.14(4)	99.85(6)	98.43(7)
O–M–Cl2	92.53(9)	103.05(4)	97.80(6)	96.20(7)
N1–M–Cl1	101.34(8)	98.72(4)	109.64(5)	102.55(6)
N1–M–Cl2	142.88(9)	150.68(4)	133.66(5)	143.93(6)
N2–M–Cl1	103.33(9)	104.73(5)	89.04(5)	88.63(5)
N2–M–Cl2	102.30(9)	103.00(4)	99.29(5)	100.46(6)
N1–M–N2	76.86(12)	75.29(6)	78.58(7)	80.76(7)
Cl1–M–Cl2	114.62(5)	109.79(2)	116.64(3)	113.50(3)

2.3. Solution polymerization of 1,3-butadiene

Ethylaluminum sesquichloriide (EASC) was proved to be more effective for cobalt complexes in the polymerization of butadiene [10,12a,17]. Therefore, the cobalt complex **2a**/EASC catalytic system was investigated under various reaction parameters to optimize the polymerization conditions, such as Al/Co molar ratio, reaction temperature and reaction time. The Al/Co molar ratio had a great influence on the catalytic activity albeit the microstructure of the resulting polymers didn't change apparently; the *cis*-1,4 content was in the range of 94.1%–96.0% along with small amounts of *trans*-1,4-PBD and 1,2-PBD. The lower concentration of EASC ([Al]/[Co] = 5) could initiate the polymerization of butadiene, affording 61.1% conversion of butadiene. The conversion of butadiene increased considerably along with the increase of Al/Co molar ratio from 5 to 40 (entries 1–5 in Table 2) and a complete conversion of butadiene was obtained under the Al/Co molar ratio of 40 in 60 min. It was observed that the molecular weight initially increased and then decreased and the highest molecular weight was obtained under the Al/Co molar ratio of 20, which was different from the case of olefin polymerization in that the chain transfer to aluminum was usually an important factor for molecular weight. However, the Al/Co molar ratio slightly affected the molecular weight distribution.

The butadiene polymerizations were also carried out over the temperature range from 0 to 90 °C at an Al/Co molar ratio of 40 with the **2a**/EASC catalytic system (entries 5–9 in Table 2). The 39.3% conversion of butadiene was gained at 0 °C; however, other cobalt-based catalytic systems gave almost no activity at 0 °C [11b,13,17]. The highest activity was observed at 25 °C with the complete conversion of butadiene. The **2a**/EASC catalytic system had remarkable thermal stability at 25–70 °C affording the 88.7% conversion of butadiene at 70 °C, but the conversion dropped sharply to 56.6% when the temperature was increased up to 90 °C probably due to the deactivation of active species at higher temperatures. The decrease in polymerization rate at the elevated reaction temperature is very common in olefin polymerization catalyzed by late-transition metal complexes [22]. The molecular weights of PBDs obtained at 0–50 °C showed only slight differences, but decreased as the temperature was increased to 70 and 90 °C. The molecular weight distributions of PBDs didn't change greatly at the different temperatures. One of the most distinguished features was the important change of polymer microstructure induced by the variation of reaction temperature. The amount of *trans*-1,4-PBDs in the polymers increased gradually along with the elevation of reaction temperature (Fig. 5). As a result, the polymerization at 90 °C produced the 12.5% content of *trans*-1,4 isomer and the *cis*-1,4 content reduced to 82.9%, which was largely different from the PBDs obtained at 25 °C containing 2.4% of *trans*-1,4 and 96.0% of *cis*-1,4 isomers. However the content of 1,2-inserted isomer slightly increased from 1.6% to 4.6% over the temperature range from 0 to 90 °C.

In order to explore the influence of ligand environment, including steric and electronic effects, on the catalytic activity and properties of resulting polymers, the butadiene polymerizations catalyzed by all the cobalt complexes (**1a**–**6a**) were carried out under similar conditions with the Al/Co molar ratio of 40 over 30 min and at 25 °C (entries 10–15 in Table 2). The substituents (R^1) on the imino- or amino-N aryl ring had an obvious influence on the catalytic performances of the cobalt complexes. The bulkier substituents led to lower conversion of butadiene and relatively higher molecular weight. The more bulkiness of the R^1 groups at the *ortho*-positions of aryl ring may to some extent prevent the access of monomer to the active center in the catalytic system, therefore resulting in the decrease of catalytic activity. For instance,

Table 2
Polymerization of 1,3-butadiene with complexes **1a**–**6a**/EASC.[a]

Entry	Cat.	Al/Co	t (min)	T (°C)	Conv. (%)	M_n[b] (10^5 g/mol)	M_w/M_n[b]	Microstructure[c] (mol%)		
								cis–1,4–	*trans*–1,4–	1,2-
1	**2a**	5	60	25	61.1	1.98	1.48	94.1	4.0	1.9
2	**2a**	10	60	25	81.9	2.18	1.47	95.3	2.8	1.9
3	**2a**	20	60	25	94.5	2.30	1.51	96.0	2.3	1.7
4	**2a**	30	60	25	97.6	1.95	1.94	95.7	2.1	2.2
5	**2a**	40	60	25	100	1.99	1.44	96.0	2.4	1.6
6	**2a**	40	60	0	39.3	2.01	1.31	95.6	1.8	2.6
7	**2a**	40	60	50	97.7	2.03	1.62	91.5	5.9	2.6
8	**2a**	40	60	70	88.7	1.64	1.43	88.1	8.6	3.3
9	**2a**	40	60	90	56.6	1.54	1.31	82.9	12.5	4.6
10	**1a**	40	30	25	93.3	2.31	1.57	96.6	1.7	1.7
11	**2a**	40	30	25	82.9	2.57	1.45	96.6	1.9	1.5
12	**3a**	40	30	25	73.2	3.08	1.50	96.3	1.8	1.9
13	**4a**	40	30	25	62.6	2.53	1.81	96.8	1.7	1.5
14	**5a**	40	30	25	90.8	2.53	1.59	96.9	1.5	1.6
15	**6a**	40	30	25	77.1	2.61	1.46	96.7	1.6	1.7
16	$CoCl_2$	40	30	25	5.6	–	–	–	–	–

[a] Polymerization conditions: precatalyst: 10.0 μmol, cocat.: EASC, solvent: toluene, total volume: 20 mL, [BD]/[Co]: 2000.
[b] Determined by GPC against polystyrene standards and reported uncorrected.
[c] Determined by ^{1}H and ^{13}C NMR spectroscopy.

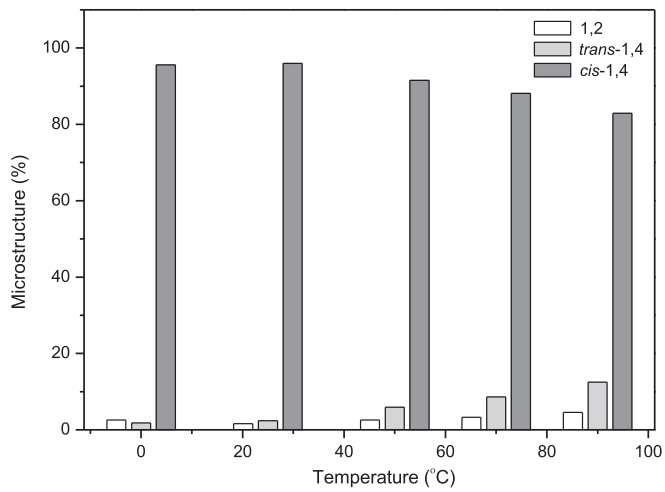

Fig. 5. Microstructure of PBDs produced by **2a**/EASC system at different temperatures (entries 5–9 in Table 2).

complex **1a** (R^1 = Me, 93.3% conv.) bearing two methyl groups on the imino-N aryl ring achieved higher conversion than complexes **2a** (R^1 = Et, 82.9% conv.) and **3a** (R^1 = *i*-Pr, 73.2% conv.) with ethyl and isopropyl groups on the imino-N aryl ring, respectively. Similarly, when comparing complexes **5a** and **6a** with amino-pyridyl alcohol ligands, **5a** (R^1 = Me, 90.8% conv.) also had much higher conversion of butadiene than **6a** (R^1 = Et, 77.1% conv.). In contrast to the catalytic activity, the molecular weights of PBDs obtained by these cobalt complexes exhibited the converse regularity (in the orders of **1a** < **2a** < **3a** and **5a** < **6a**). In the same way, the substituents (R) on the HO–C atom had an important influence on the catalytic performance. On replacing two hydrogen atoms by two methyl groups on the HO–C atom, complex **4a** (62.6%) obtained much lower conversion of butadiene than the corresponding complex **2a** (82.9%). After the imino groups were reduced to amino groups in the ligands, slightly lower conversions of butadiene were observed by comparison with **1a** and **5a**, **2a** and **6a** (conversion orders: **1a** > **5a**; **2a** > **6a**). The PBDs produced by complexes **1a**–**6a** had very similar microstructure with high *cis*-1,4 contents (96.3%–96.9%) and narrow molecular weight distributions (1.45–1.81) in spite of their different molecular weights.

The nature of the metal center had a large influence on the catalytic performance. In general, cobalt-based catalysts were more active than the corresponding nickel-based analogs; under the similar conditions employed here, nickel complex **2b**/EASC system gained much lower conversion of butadiene (27.2%) than cobalt complex **2a** with the same ligand (82.9%), although the conversion increased to 61.1% after 2 h (entry 11 in Table 2 and entry 2–3 in Table 3). The metal center also greatly influenced the molecular weight, molecular weight distribution and stereoregularity of the resulting polymers. All the nickel complexes **1b**–**6b** yielded much lower molecular weights (6000–7150 g/mol), broader molecular weight distributions (3.42–4.25), and lower *cis*-1,4 contents (91.5%–91.8%) than the cobalt complexes **1a**–**6a** sharing the same corresponding ligand environments. Similarly, as for the nickel complexes, the more bulkiness of the R^1 groups at the *ortho*-positions of the imino- or amino-N aryl ring also resulted in the lower conversion of butadiene (in the orders of **1b** > **2b** > **3b** and **5b** > **6b**); whereas the influence was relatively smaller than that on the corresponding cobalt complexes. The substituents (R) on the HO–C atom had more important influence on the catalytic activity. Nickel complex **4b** with two methyl groups produced higher conversion of butadiene than **2b** with CH_2OH group on the HO–C atom. On the contrary, nickel complexes **5b** and **6b** with amino groups in the ligands were more active than the corresponding nickel complexes **1b** and **2b** with imino groups (conversion orders: **1b** < **5b**; **2b** < **6b**). The results in Table 3 demonstrated that the ligand environment didn't significantly influence molecular weight, molecular weight distribution and microstructure of the obtained polymers. The microstructure of PBDs produced by nickel complexes was also found to be mainly *cis*-1,4-PBD together with small amounts of *trans*-1,4 and 1,2-vinyl isomers although the *cis*-1,4 contents were lower than those afforded by cobalt complexes (Fig. 6).

Table 3
Polymerization of 1,3-butadiene with complexes **1b**–**6b**/EASC.[a]

Entry	Cat.	Conv. (%)	M_n[b] (10^3 g/mol)	M_w/M_n[b]	Microstructure[c] (mol%)		
					cis–1,4–	*trans*–1,4–	1,2-
1	**1b**	67.9	7.15	3.42	91.7	5.5	2.8
2[d]	**2b**	27.2	9.36	3.18	91.4	5.0	3.6
3	**2b**	61.1	6.74	3.74	91.6	5.3	3.1
4	**3b**	59.2	6.06	4.25	91.8	5.0	3.2
5	**4b**	76.2	6.17	3.76	91.5	6.6	1.9
6	**5b**	75.3	6.34	3.69	91.6	6.0	2.4
7	**6b**	68.6	6.00	4.08	91.7	5.4	2.9
8	$NiCl_2$	16.4	–	–	–	–	–

[a] Polymerization conditions: precatalyst: 10.0 μmol, cocat.: EASC, [Al]/[Ni]: 40, solvent: toluene, total volume: 20 mL, [BD]/[Ni]: 2000, reaction temperature: 25 °C; reaction time: 2 h.
[b] Determined by GPC against polystyrene standards and reported uncorrected.
[c] Determined by ^1H and ^{13}C NMR spectroscopy.
[d] Reaction time: 30 min.

3. Conclusions

A series of cobalt(II) and nickel(II) complexes ligated by imino- or amino-pyridyl alcohol ligands (**L1**–**L6**) were synthesized and characterized. All the complexes adopted distorted trigonal bipyramidal configuration with the equatorial plane formed by the pyridyl nitrogen atoms and two chlorine atoms conformed by single-crystal X-ray analysis. Upon activation with EASC, all the cobalt complexes **1a**–**6a** obtained *cis*-1,4-polybutadiene with high activity and selectivity (>96%) under the reaction conditions employed here. The increase of Al/Co molar ratio enhanced the conversion of butadiene and the catalytic system kept active over the wide temperature

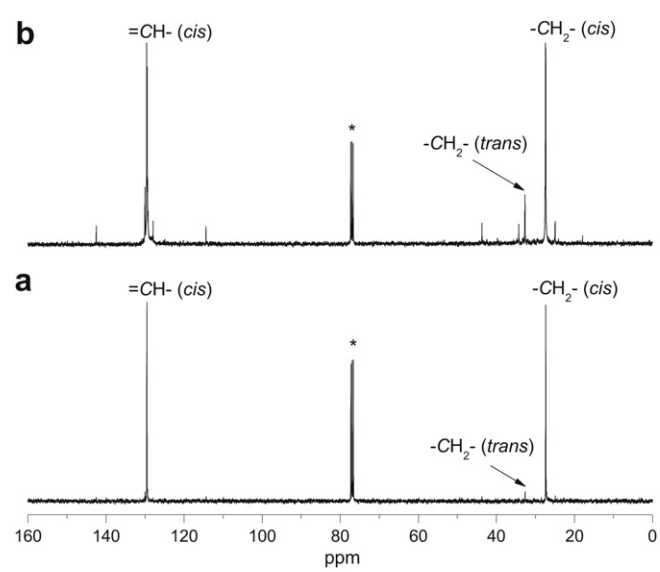

Fig. 6. The ^{13}C NMR of PBDs obtained by **2a**/EASC (a, entry 11 in Table 2) and **2b**/EASC (b, entry 3 in Table 3). *, $CDCl_3$.

range of 0–90 °C. However the reaction temperature importantly influenced the microstructure of the resulting polymers. The difference of ligand environment led to the variation of catalytic activity although it didn't affect the *cis*-1,4 content of PBDs greatly. In contrast to cobalt complexes, the corresponding nickel complexes **1b**–**6b** bearing the same ligands yielded lower conversion of butadiene, *cis*-1,4 content and molecular weight, and broader molecular weight distribution under the similar reaction conditions. The polymerization reactions with $CoCl_2$ or $NiCl_2$/EASC systems produced remarkably lower conversions, elucidating the importance of ligand influence to the active centers.

4. Experimental

4.1. General considerations and materials

All manipulations of air- or moisture-sensitive compounds were carried out under an atmosphere of nitrogen using standard Schlenk techniques. FT-IR spectra were recorded on a Perkin–Elmer FT-IR 2000 spectrometer by using KBr disks in the range 4000–400 cm^{-1} ^1H NMR and ^{13}C NMR spectra were recorded on a Bruker DMX-400 instrument in $CDCl_3$ with TMS as the internal standard. Splitting patterns are designated as follows: s, singlet; d, doublet; dd, double doublet; t, triplet; q, quadruplet; sept, septet; m, multiplet. Elemental analysis was performed on a Flash EA1112 microanalyzer. The molecular weight and molecular weight distribution of polybutadienes were measured by GPC using Waters 2414 series system in THF at 25 °C calibrated with polystyrene standards.

Toluene and tetrahydrofuran were refluxed over sodium-benzophenone and distilled under nitrogen prior to use. Ethylaluminum sesquichloride (EASC, 0.4 M in hexane) and all the anilines were purchased from Acros Chemicals. Methyl lithium (1.0 M in THF) was purchased from Jingyan Chemicals (Shanghai) co., Ltd. $NiC1_2 \cdot 6H_2O$, $CoCl_2 \cdot 6H_2O$ and sodium borohydride were obtained from Beijing Chemical Regents Co. and directly used without further purification. Polymerization grade butadiene was purified by passing it through columns of KOH and molecular sieves. All other chemicals were obtained commercially and used without further purification unless otherwise stated. The compounds, 2-COOEt-6-(2,6-$R^1{}_2C_6H_3N{=}CMe)C_5H_3N$ (R^1 = Me, **1**; Et, **2**; *i*-Pr, **3**) [19] and the ligands, 2-(2,6-*i*-$Pr_2C_6H_3N{=}CMe)$-6-$(CH_2OH)C_5H_3N$ (**L3**) [20,21] and 2-(2,6-$Et_2C_6H_3N{=}CMe)$-6-$\{(HO)CMe_2\}C_5H_3N$ (**L4**) [18] were prepared according to the literature.

4.2. Synthesis of ligands (*L1*, *L2*, *L5*, *L6*)

4.2.1. 2-(2,6-$Me_2C_6H_3N{=}CMe)$-6-$(CH_2OH)C_5H_3N$ (*L1*)

To a methanol solution (50 mL) containing compound **1** (0.7352 g, 2.48 mmol) and anhydrous calcium chloride (0.5658 g, 5.10 mmol), was slowly added 1.1 equivalent of sodium borohydride (0.1034 g, 2.73 mmol) at 0 °C. The reaction solution was slowly warmed to room temperature and then refluxed for 8 h. After the solution was cooled to room temperature, distilled water was added and methanol was removed under reduced pressuere. The resulting solution was then extracted with chloroform (30 mL × 3), and the combined organic extracts were dried over anhydrous Na_2SO_4 and filtered. After all the volatiles were removed under reduced pressure, the resultant crude product was purified on a silica column (petroleum ether/ethyl acetate = 5:1) to give **L1** as yellow sticky oil (yield: 0.4764 g, 75.5%). FT-IR (liquid film, cm^{-1}): 3356 (ν_{O-H}), 2962, 2920, 2852, 1645 ($\nu_{C=N}$), 1587, 1464, 1441, 1364, 1308, 1260, 1203, 1112, 1090, 1059, 1025, 801, 769. ^1H NMR (400 MHz, $CDCl_3$), δ (ppm): 8.29 (d, 1 H, J = 7.6 Hz, py–*H*), 7.81 (t, 1 H, J = 7.6 Hz, py–*H*), 7.32 (d, 1 H, J = 7.6 Hz, py–*H*), 7.07 (d, 2 H, J = 7.6 Hz, Ar–*H*), 6.94 (t, 1 H, J = 7.6 Hz, Ar–*H*), 4.83 (s, 2 H, CH_2OH), 3.99 (b, 1 H, O*H*), 2.20 (s, 3 H, $CH_3C{=}N$), 2.03 (s, 6 H, Ar–CH_3). ^{13}C NMR (125 MHz, $CDCl_3$), δ (ppm): 166.7 (*C*=N), 157.6, 155.0, 148.4, 137.2, 127.9, 125.4, 123.1, 121.5, and 119.9 (py–*C* and aromatic-*C*), 63.7 (CH_2OH), 17.9 (Ar–CH_3), 16.6 ($CH_3C{=}N$). Anal. Calcd. for $C_{16}H_{18}N_2O$ (254.33): C, 75.56; H, 7.13; N, 11.01. Found: C, 74.55; H, 7.41; N, 10.55.

4.2.2. 2-(2,6-$Et_2C_6H_3N{=}CMe)$-6-$(CH_2OH)C_5H_3N$ (*L2*)

By using the same procedure described for **L1**, ligand **L2** was obtained from compound **2** (0.9258 g, 2.85 mmol) and $NaBH_4$ (0.1175 g, 3.11 mmol) as yellow sticky oil (yield: 0.6403 g, 79.5%). FT-IR (liquid film, cm^{-1}): 3411 (ν_{O-H}), 2965, 2931, 2873, 1644 ($\nu_{C=N}$), 1582, 1451, 1365, 1309, 1260, 1196, 1110, 1059, 1024, 801, 771. FT-IR (KBr disk, cm^{-1}): 3430 (ν_{O-H}), 3063, 2965, 2931, 2873, 1644 ($\nu_{C=N}$), 1582, 1451, 1365, 1309, 1260, 1226, 1196, 1151, 1110, 1059, 801, 771. ^1H NMR (400 MHz, $CDCl_3$), δ (ppm): 8.29 (d, 1 H, J = 7.6 Hz, py–*H*), 7.82 (t, 1 H, J = 7.6 Hz, py–*H*), 7.32 (d, 1 H, J = 7.6 Hz, py–*H*), 7.11 (d, 2 H, J = 7.6 Hz, Ar–*H*), 7.06–7.02 (m, 1 H, Ar–*H*), 4.84 (s, 2 H, CH_2OH), 3.99 (b, 1 H, O*H*), 2.43–2.31 (m, 4 H, CH_2CH_3), 2.22 (s, 3 H, $CH_3C{=}N$), 1.14 (t, 6 H, J = 7.6 Hz, CH_2CH_3). ^{13}C NMR (125 MHz, $CDCl_3$), δ (ppm): 166.4 (*C*=N), 157.6, 155.0, 147.5, 137.2, 131.1, 125.9, 123.4, 121.5, and 119.9 (py–*C* and aromatic-*C*), 63.7 (CH_2OH), 24.5 (CH_2CH_3), 17.0 ($CH_3C{=}N$), 13.7 (CH_2CH_3). Anal. Calcd for $C_{18}H_{22}N_2O$ (282.38): C, 76.56; H, 7.85; N, 9.92. Found: C, 75.32; H, 8.00; N, 10.05.

4.2.3. 2-(2,6-$Me_2C_6H_3NHCHMe)$-6-$(CH_2OH)C_5H_3N$ (*L5*)

To a methanol solution (50 mL) containing compound **1** (0.8285 g, 2.80 mmol) and anhydrous calcium chloride (1.2430 g, 11.20 mmol), was slowly added 4.0 equivalents of sodium borohydride (0.4297 g, 11.36 mmol) at 0 °C. The reaction solution was slowly warmed to room temperature and then refluxed for 24 h. After the solution was cooled to room temperature, distilled water was added and methanol was removed under reduced pressure. The resulting solution was then extracted with chloroform (30 mL × 3), and the combined organic extracts were dried over anhydrous Na_2SO_4 and filtered. After all the volatiles were removed under reduced pressure, the resultant crude product was purified on a silica column (petroleum ether/ethyl acetate = 5:1) to give **L1** (the first eluting part; yield: 0.2460 g, 34.6%) and **L5** as an off-white solid (the second eluting part; yield: 0.4686 g, 65.4%). FT-IR (KBr disk, cm^{-1}): 3360 ($\nu_{O-H,\ N-H}$), 2968, 2924, 2858, 1593, 1574, 1469, 1449, 1370, 1261, 1219, 1154, 1121, 1091, 1030, 993, 800, 764, 669. ^1H NMR (400 MHz, $CDCl_3$), δ (ppm): 7.57 (t, 1 H, J = 7.6 Hz, py–*H*), 7.08 (d, 1 H, J = 7.6 Hz, py–*H*), 7.02 (d, 1 H, J = 7.6 Hz, py–*H*), 6.94 (d, 2 H, J = 7.2 Hz, Ar–*H*), 6.77 (t, 1 H, J = 7.4 Hz, Ar–*H*), 4.76 (s, 2 H, CH_2OH), 4.45 (q, 1 H, J = 6.8 Hz, CH_3CHNH), 3.99 (s, 1 H, N*H*), 3.94 (s, 1 H, O*H*), 2.23 (s, 6 H, Ar–CH_3), 1.49 (d, 3 H, J = 6.8 Hz, CH_3CH). ^{13}C NMR (125 MHz, $CDCl_3$), δ (ppm): 162.3, 158.3, 144.6, 137.2, 129.1, 128.8, 121.5, 120.0, and 118.7 (py–*C* and aromatic-*C*), 63.8 (CH_2OH), 57.4 (*C*HNH), 22.3 (CH_3CH), 18.9 (Ar–CH_3). Anal. Calcd for $C_{16}H_{20}N_2O$ (256.34): C, 74.97; H, 7.86; N, 10.93. Found: C, 74.47; H, 7.74; N, 11.20.

4.2.4. 2-(2,6-$Et_2C_6H_3NHCHMe)$-6-$(CH_2OH)C_5H_3N$ (*L6*)

By using the same procedure described for **L5**, ligand **L6** was obtained from compound **2** (0.7960 g, 2.45 mmol) and $NaBH_4$ (0.4655 g, 12.30 mmol) as an off-white solid (yield: 0.4096 g, 58.7%). FT-IR (KBr disk, cm^{-1}): 3364 ($\nu_{O-H,\ N-H}$), 2965, 2930, 2873, 1593, 1576, 1455, 1368, 1262, 1202, 1154, 1121, 1087, 797, 754. ^1H NMR (400 MHz, $CDCl_3$), δ (ppm): 7.57 (t, 1 H, J = 7.6 Hz, py–*H*), 7.09 (d, 1 H, J = 7.6 Hz, py–*H*), 7.03–7.00 (m, 3 H, 1 py–*H* and 2 Ar–*H*), 6.91 (t, 1 H, J = 7.6 Hz, Ar–*H*), 4.77 (d, 2 H, J = 4.0 Hz, CH_2OH), 4.39 (q, 1 H, J = 6.8 Hz, CH_3CHNH), 4.14 (s, 1 H, N*H*), 3.94 (t, 1 H, J = 4.4 Hz, O*H*), 2.61 (q, 4 H, J = 7.6 Hz, CH_2CH_3), 1.47 (d, 3 H, J = 6.8 Hz, CH_3CH), 1.21 (t, 6 H, J = 7.6 Hz, CH_2CH_3). ^{13}C NMR (125 MHz, $CDCl_3$), δ (ppm): 162.2, 158.3, 143.4, 137.1, 135.7, 126.4, 122.1, 120.0, and 118.7 (py–*C*

and aromatic-*C*), 63.8(*C*H$_2$OH), 58.5 (*C*HNH), 24.5 (*C*H$_2$CH$_3$), 22.1 (*C*H$_3$CH), 14.4 (CH$_2$*C*H$_3$). Anal. Calcd for $C_{18}H_{24}N_2O$ (284.40): C, 76.02; H, 8.51; N, 9.85. Found: C, 76.37; H, 8.51; N, 9.85.

4.3. Preparation of cobalt and nickel complexes

4.3.1. General procedure

To a stirred solution of the corresponding ligand (0.50 mmol) in anhydrous ethanol (20 mL), one equivalent of $CoCl_2 \cdot 6H_2O$ or $NiCl_2 \cdot 6H_2O$ (0.50 mmol) was added, and the reaction mixture was stirred at room temperature overnight. The resultant solution was concentrated to ca. 3 mL. Diethyl ether was added to precipitate the product, which was filtered, washed repeatedly with diethyl ether and dried under vacuum. All of the complexes were prepared in high yield in this manner.

4.3.2. Synthesis of cobalt complexes **1a**–**6a**

1a: Green powder in 62.1% yield. FT-IR (KBr disk, cm^{-1}): 3379, 3090, 2976, 2915, 1618 ($\nu_{C=N}$), 1593, 1473, 1455, 1441, 1371, 1291, 1204, 1094, 1049, 798, 781. Anal. Calcd for $C_{16}H_{18}Cl_2CoN_2O$ (384.17): C, 50.02; H, 4.72; N, 7.29. Found: C, 49.98; H, 4.54; N, 6.90. **2a**: Green powder in 86.0% yield. FT-IR (KBr disk, cm^{-1}): 3267, 3073, 2966, 2930, 2873, 1624 ($\nu_{C=N}$), 1598, 1471, 1451, 1370, 1295, 1199, 1044, 1027, 802, 771. Anal. Calcd for $C_{18}H_{22}Cl_2CoN_2O$ (412.22): C, 52.45; H, 5.38; N, 6.80. Found: C, 52.66; H, 5.23; N, 6.51. **3a**: Green powder in 94.5% yield. FT-IR (KBr disk, cm^{-1}): 3252, 2964, 2923, 2868, 1618 ($\nu_{C=N}$), 1592, 1468, 1458, 1439, 1385, 1372, 1322, 1296, 1195, 1057, 1028, 811, 797, 781. Anal. Calcd for $C_{20}H_{26}Cl_2CoN_2O$ (440.27): C, 54.56; H, 5.95; N, 6.36. Found: C, 54.58; H, 5.71; N, 6.36. **4a**: Light green powder in 94.5% yield. FT-IR (KBr disk, cm^{-1}): 3409, 3256, 3066, 2975, 2936, 2875, 1619 ($\nu_{C=N}$), 1590, 1467, 1458, 1450, 1375, 1351, 1325, 1288, 1258, 1210, 1171, 1136, 1095, 1023, 820, 802. Anal. Calcd for $C_{20}H_{26}Cl_2CoN_2O$ (440.27): C, 54.56; H, 5.95; N, 6.36. Found: C, 54.54; H, 5.84; N, 6.32. **5a**: Deep blue powder in 96.8% yield. FT-IR (KBr disk, cm^{-1}): 3324, 3298, 2974, 2926, 1606, 1578, 1471, 1453, 1417, 1371, 1283, 1192, 1162, 1129, 1101, 1044, 974, 882, 823, 801, 788. Anal. Calcd for $C_{16}H_{20}Cl_2CoN_2O$ (386.18): C, 49.76; H, 5.22; N, 7.25. Found: C, 49.31; H, 5.33; N, 7.14. **6a**: Deep blue powder in 81.1% yield. FT-IR (KBr disk, cm^{-1}): 3312, 3221, 2968, 2932, 2871, 1607, 1579, 1474, 1454, 1421, 1377, 1293, 1170, 1130, 1044, 964, 925, 855, 825, 795. Anal. Calcd for $C_{18}H_{24}Cl_2CoN_2O$ (414.24): C, 52.19; H, 5.84; N, 6.76. Found: C, 51.79; H, 5.72; N, 6.71.

4.3.3. Synthesis of nickel complexes **1b**–**6b**

1b: Brick-red powder in 91.1% yield. FT-IR (KBr disk, cm^{-1}): 3366, 3227, 2917, 1617 ($\nu_{C=N}$), 1590, 1471, 1440, 1374, 1299, 1267, 1207, 1097, 1041, 841, 792. Anal. Calcd for $C_{16}H_{18}Cl_2N_2NiO$ (383.93): C, 50.05; H, 4.73; N, 7.30. Found: C, 49.75; H, 4.43; N, 7.08. **2b**: Brick-red powder in 94.3% yield. FT-IR (KBr disk, cm^{-1}): 3386, 3223, 3076, 2969, 2932, 2876, 1621 ($\nu_{C=N}$), 1596, 1447, 1371, 1297, 1201, 1102, 1039, 801, 773. Anal. Calcd for $C_{18}H_{22}Cl_2N_2NiO$ (411.98): C, 52.48; H, 5.38; N, 6.80. Found: C, 52.39; H, 5.11; N, 6.72. **5b**: Yellowish brown powder in 85.2% yield. FT-IR (KBr disk, cm^{-1}): 3320, 3163, 2977, 2931, 1604, 1579, 1473, 1375, 1283, 1191, 1162, 1129, 1098, 1036, 982, 937, 901, 806. Anal. Calcd for $C_{16}H_{20}Cl_2N_2NiO$ (385.94): C, 49.79; H, 5.22; N, 7.26. Found: C, 49.42; H, 4.98; N, 7.07. **6b**: Yellowish brown powder in 72.6% yield. FT-IR (KBr disk, cm^{-1}): 3288, 3219, 2968, 2932, 2872, 1609, 1583, 1453, 1418, 1379, 1290, 1249, 1169, 1129, 1041, 973, 933, 796. Anal. Calcd for $C_{18}H_{24}Cl_2N_2NiO$ (414.00): C, 52.22; H, 5.84; N, 6.77. Found: C, 51.89; H, 5.70; N, 6.58.

4.4. Polymerization of 1,3-butadiene

Solution polymerizations of 1,3-butadiene in toluene were carried out in a sealed glass reactor (100 mL) with a rubber septum and a connection to a vacuum system. The reactor was charged with the desired amounts of precatalyst and cocatalyst solutions. The mixture was stirred for 2 min at the desired temperature and

Table 4
Crystallographic data and refinement parameters for complexes **2a**, **4a**, **6a** and **6b**.

	2a	**4a**	**6a**	**6b**
Formula	$C_{18}H_{22}Cl_2CoN_2O$	$C_{20}H_{26}Cl_2CoN_2O$	$C_{18}H_{24}Cl_2CoN_2O$	$C_{18}H_{24}Cl_2N_2NiO$
Formula weight	412.21	440.26	414.22	414.00
Temp. (K)	293(2)	293(2)	293(2)	293(2)
Wavelength (Å)	0.71073	0.71073	0.71073	0.71073
Crystal system	Triclinic	Monoclinic	Monoclinic	Monoclinic
Space group	P−1	P2(1)/n	P2(1)/c	P2(1)/c
a (Å)	7.2885(15)	8.3666(17)	8.2399(16)	8.4036(17)
b (Å)	9.0459(18)	12.386(3)	14.804(3)	14.531(3)
c (Å)	16.274(3)	20.052(4)	15.856(3)	15.764(3)
α (°)	75.73(3)	90.00	90.00	90.00
β (°)	82.62(3)	91.32(3)	97.59(3)	98.53(3)
γ (°)	69.89(3)	90.00	90.00	90.00
Volume (Å^3)	975.3(3)	2077.5(7)	1917.2(7)	1903.7(7)
Z	2	4	4	4
D_{calc} (Mg m^{-3})	1.404	1.408	1.435	1.444
μ (mm^{-1})	1.160	1.094	1.181	1.307
F(000)	426	916	860	864
Crystal size(mm)	0.39 × 0.24 × 0.10	0.40 × 0.28 × 0.20	0.39 × 0.28 × 0.24	0.48 × 0.39 × 0.33
θ range (°)	3.01–27.42	3.09–27.42	2.99–27.41	3.09–27.40
Limiting indices	$-9 \le h \le 9, -11 \le k \le 11, -21 \le l \le 21$	$-10 \le h \le 9, -16 \le k \le 16, -25 \le l \le 25$	$-9 \le h \le 10, -19 \le k \le 18, -20 \le l \le 20$	$-10 \le h \le 10, -18 \le k \le 18, -20 \le l \le 18$
No. of rflns collected	9668	19645	18150	17224
No. of unique rflns	4423	4715	4358	4281
No. of obsd rflns($I > 2\sigma(I)$)	2834	3736	3233	3539
Completeness to θ (%)	0.992 ($\theta = 27.42°$)	0.998 ($\theta = 27.42°$)	0.998 ($\theta = 27.41°$)	98.8 ($\theta = 27.40°$)
No. of parameters	208	236	219	219
Goodness-of-fit on F^2	1.121	1.081	1.084	1.083
Final R indices [$I > 2\sigma(I)$]	$R_1 = 0.0413$, $wR_2 = 0.1058$	$R_1 = 0.0283$, $wR_2 = 0.0689$	$R1 = 0.0348$, $wR2 = 0.0810$	$R_1 = 0.0378$, $wR_2 = 0.0977$
R indices(all data)	$R_1 = 0.0766$, $wR_2 = 0.1406$	$R_1 = 0.0413$, $wR_2 = 0.0776$	$R_1 = 0.0523$, $wR_2 = 0.0898$	$R_1 = 0.0468$, $wR_2 = 0.1027$
largest diff peak, hole (e Å^{-3})	0.754, −0.593	0.305, −0.247	0.357, −0.366	0.544, −0.514

followed by the addition of a solution of 1,3-butadiene in toluene. The polymerization reaction was carried out by vigorous stirring of the reaction mixture at the various temperatures. After the polymerization, the resulting solution was poured into a large amount of acidified ethanol (5% v/v solution of HCl) containing 2,6-di-*tert*-butyl-4-methylphenol as a stabilizer. The precipitated polymers were filtered, washed with ethanol and dried under vacuum at 50 °C overnight.

4.5. X-ray crystallography measurements

Single-crystal X-ray diffraction studies for **2a**, **4a**, **6a** and **6b** were carried out on a Rigaku RAXIS Rapid IP diffractometer with graphite monochromated Mo–K_α radiation ($\lambda = 0.71073$ Å). Cell parameters were obtained by global refinement of the positions of all collected reflections. Intensities were corrected for Lorentz and polarization effects and empirical absorption. The structures were solved by direct methods and refined by full-matrix least-squares on F^2. All non-hydrogen atoms were refined anisotropically. All hydrogen atoms were placed in calculated positions. Structure solution and refinement were performed by using the SHELXL-97 Package [23]. Crystallographic data and processing parameters for complexes **2a**, **4a**, **6a** and **6b** are summarized in Table 4.

Acknowledgments

This work was supported by the National Natural Science Foundation of China (Grant No. 21006085) and the State Key Laboratory of Chemical Engineering (Grant No. SKL-ChE-11D03).

Appendix A. Supplementary material

CCDC 855903(**2a**), 855904(**4a**), 855905(**6a**) and 855906(**6b**) contain the supplementary crystallographic data for this paper. These data can be obtained free of charge from the Cambridge Crystallographic Data Center via www.ccdc.cam.ac.uk/data_request/cif.

References

[1] (a) L. Porri, A. Giamsso, Part II, In: Conjugated Diene Polymerization in Comprehensive Polymer Science, vol. 4, Pergamon, Oxford, 1989, pp. 53–108;
(b) L. Porri, A. Giarrusso, G. Ricci, Prog. Polym. Sci. 16 (1991) 405–441;
(c) R. Taube, G. Sylvester, Applied Homogeneous Catalysis with Organometallic Complexes, Wiley-VCH, Weinheim, Germany, 2002, pp. 285–315;
(d) S.K.-H. Thiele, D.R. Wilson, J. Macromol. Sci. Part C: Polym. Rev. C43 (2003) 581–628.
[2] G.J. Van Amerongen, Adv. Chem. Ser. 52 (1966) 136–152.
[3] W. Cooper, Ind. Eng. Chem. Prod. Res. Develop. 9 (1970) 457–466.
[4] (a) J. Furukawa, Pure Appl. Chem. 42 (1975) 495–508;
(b) J. Furukawa, Acc. Chem. Res. 13 (1980) 1–6.
[5] A. Oehme, U. Gebauer, K. Gehrke, M.D. Lechner, Angew. Makromol. Chem. 235 (1996) 121–130.
[6] (a) K. Endo, N. Hatakeyama, J. Polym. Sci. Part A: Polym. Chem. 39 (2001) 2793–2798;
(b) D.C.D. Nath, T. Shiono, T. Ikeda, Macromol. Chem. Phys. 203 (2002) 756–760;
(c) D.C.D. Nath, T. Shiono, T. Ikeda, Appl. Catal. A: Gen. 238 (2003) 193–199;
(d) G. Kwag, C. Bae, S. Kim, J. Appl. Polym. Sci. 113 (2009) 2186–2190;
(e) Z. Cai, M. Shinzawa, Y. Nakayama, T. Shiono, Macromolecules 42 (2009) 7642–7643.
[7] (a) G. Leone, A. Boglia, F. Bertini, M. Canetti, G. Ricci, J. Polym. Sci. Part A: Polym. Chem. 48 (2010) 4473–4483;
(b) G. Ricci, A. Sommazzi, F. Masi, M. Ricci, A. Boglia, G. Leone, Coord. Chem. Rev. 254 (2010) 661–676 (and references therein).
[8] K. Schroder, K. Gehrke, Macromol. Chem. Rapid Commun. 13 (1992) 571–575.
[9] K. Endo, T. Kitagawa, K. Nakatani, J. Polym. Sci. Part A: Polym. Chem. 44 (2006) 4088–4094.
[10] D. Chandran, C.H. Kwak, C.S. Ha, I. Kim, Catal. Today 131 (2008) 505–512.
[11] (a) K.B. Ung, J.S. Kim, K.J. Lee, C.S. Ha, I. Kim, Stud. Surf. Sci. Catal. 159 (2006) 873–876;
(b) D. Gong, B. Wang, C. Bai, J. Bi, F. Wang, W. Dong, X. Zhang, L. Jiang, Polymer 50 (2009) 6259–6264;
(c) D. Gong, B. Wang, H. Cai, X. Zhang, L. Jiang, J. Organomet. Chem. 696 (2011) 1584–1590.
[12] (a) V. Appukuttan, L. Zhang, C.S. Ha, I. Kim, Polymer 50 (2009) 1150–1158;
(b) R. Cariou, J. Chirinos, V.C. Gibson, G. Jacobsen, A.K. Tomov, M.R.J. Elsegood, Macromolecules 42 (2009) 1443–1444;
(c) R. Cariou, J.J. Chirinos, V.C. Gibson, G. Jacobsen, A.K. Tomov, G.J.P. Britovsek, A.J.P. White, Dalton Trans. 39 (2010) 9039–9045.
[13] V. Appukuttan, L. Zhang, J.Y. Ha, D. Chandran, B.K. Bahuleyan, C.-S. Ha, I. Kim, J. Mol. Catal. A: Chem. 325 (2010) 84–90.
[14] G. Kwag, Y. Jang, H. Lee, Polym. J. 31 (1999) 1274–1276.
[15] H. Suzuki, S. Matsumura, Y. Satoh, K. Sogoh, H. Yasuda, React. Funct. Polym. 59 (2004) 253–266.
[16] Y. Jang, D.S. Choi, S. Han, J. Polym. Sci. Part A: Polym. Chem. 42 (2004) 1164–1173.
[17] S. Jie, P. Ai, B.-G. Li, Dalton Trans. 40 (2011) 10975–10982.
[18] S. Jie, P. Ai, Q. Zhou, B.-G. Li, J. Organomet. Chem. 696 (2011) 1465–1473.
[19] W.-H. Sun, X. Tang, T. Gao, B. Wu, W. Zhang, H. Ma, Organometallics 23 (2004) 5037–5047.
[20] V.C. Gibson, C. Redshaw, G.A. Solan, A.J.P. White, D.J. Williams, Organometallics 26 (2007) 5119–5123.
[21] W. Zhang, S. Katao, W.-H. Sun, K. Nomura, Organometallics 28 (2009) 1558–1568.
[22] (a) C. Bianchini, G. Giambastiani, I.G. Rios, G. Mantovani, A. Meli, A.M. Segarra, Coord. Chem. Rev. 250 (2006) 1391–1418 (and references therein);
(b) V.C. Gibson, C. Redshaw, G.A. Solan, Chem. Rev. 107 (2007) 1745–1776 (and references therein);
(c) C. Bianchini, G. Giambastiani, L. Luconi, A. Meli, Coord. Chem. Rev. 254 (2010) 431–455 (and references therein).
[23] G.M. Sheldrick, SHELXTL-97, Program for the Refinement of Crystal Structures, University of Gottingen, Germany, 1997.